View metadata, citation and similar papers at core.ac.uk

brought to you by CORE

provided by Elsevier - Publisher Connector

Trapping Electrophoresis and Ratchets: A Theoretical Study for DNA-Protein Complexes

Claude Desruisseaux,*# Gary W. Slater,# and Tarso B. L. Kist#§

*Department of Biology and #Department of Physics, University of Ottawa, Ottawa, Ontario, Canada, and §Departamento de Biofísica, Universidade Federal do Rio Grande do Sul, Porto Alegre, RS, Brazil

ABSTRACT Recently, Griess and Serwer (1998. *Biophys. J.* 74:A71) showed that it was possible to use trapping electrophoresis and unbiased but asymmetrical electric field pulses to build a correlation ratchet that would allow the efficient separation of naked DNAs from identical DNAs that form a complex with a bulky object such as a protein. Here we present a theoretical investigation of this novel macromolecular separation process. We start by looking at the general features of this electrophoretic ratchet mechanism in the zero-frequency limit. We then examine the effects of finite frequencies on velocity and diffusion. Finally, we use the biased reptation model and computer simulations to understand the band-broadening processes. Our study establishes the main experimental regimes that can provide good resolution for specific applications.

INTRODUCTION

When a particle moves in an asymmetrical but periodic potential under the action of nonequilibrium fluctuations, a net drift can be observed, even though the net applied force is zero (Magnasco, 1993). Similar effects can be observed for asymmetrical fluctuations and symmetrical potentials (Chialvo and Millonas, 1995), or for various schemes in which the potential itself is fluctuating (Astumian, 1997). These systems are often referred to as correlation ratchets (CRs). Such thermodynamic systems have attracted a lot of attention recently as a model for molecular motors (Duke et al., 1995; Jülicher et al., 1997). Applications to the field of separation science have also been proposed. For example, Rousselet et al. (1994) have reported the successful (albeit inefficient) separation of particles using a simple electrostatic potential with no net force. Slater et al. (1997) proposed a system in which asymmetrical steric interactions may be used to separate macromolecules based solely on their internal entropy. Chacron and Slater (1997) suggested an electrophoresis system in which a correlation ratchet uses a strong field gradient to force the migration of the molecules toward unique fixed (spatial) points where the resulting bands self-focus (much like for isoelectrofocusing of proteins).

Gel electrophoresis is the main separation tool of modern molecular biology laboratories (Andrews, 1986). For example, current DNA sequencing and mapping methods are based entirely on the capacity of gel electrophoresis to separate DNA fragments that differ in size by less than 1%. Proteins are also routinely separated by gel electrophoresis (Guttman, 1996; Dunn and Corbett, 1996). One early example of a simple CR-like electrophoretic process was ZIFE (for zero-integrated field electrophoresis) (Turmel et al., 1990). In this process, an unbiased (average field is zero) pulsed field is applied, with short high-field pulses of intensity ϵ_H alternating with longer low-field pulses of intensity $-\epsilon_L$ (see Fig. 1). Because of the nonlinearities (the electrophoretic mobility μ of DNA increases with field intensity), a large DNA molecule acquires a finite velocity, in the direction of the high field pulses, despite the absence of a net (integrated) external applied field.

A simple ratchet process can also be constructed for large spherical particles being electrophoresed in tight gels. Indeed, it is well known that a large particle quickly becomes trapped (stops moving) in a tight gel if the field ϵ is too high (i.e., if it exceeds some trapping critical value ϵ_T; Griess and Serwer, 1990; Serwer and Griess, 1993). This is apparently due to the fact that the field drives such a particle into a dead end, where it stays trapped for an extended period of time (Griess and Serwer, 1990). If the field is low enough ($\epsilon < \epsilon_T$), the Brownian motion eventually frees the particle from the trap and the migration resumes. ZIFE-like pulses, where we alternate between a high ($\epsilon > \epsilon_T$) and a reverse low ($\epsilon < \epsilon_T$) field, will clearly lead to a net motion in the direction of the low field intensity for this system. Note that ZIFE pulses actually force particles and DNA molecules to move in opposite directions.

Ulanovsky et al. (1990) suggested attaching a bulky object (protein streptavidin in the original paper) to one end of the DNA molecule before electrophoresis to increase the separation between different DNA sizes. The idea is simple: whereas the protein's size is responsible for the trapping in dead ends, it is the electric force on the DNA molecule (hence the DNA charge) that restricts the escape from the traps. Therefore, larger DNA molecules are trapped for longer periods of time, and their mobility is more severely reduced. This process is called trapping electrophoresis (TE). The original experimental results were promising (Ulanovsky et al., 1990), but theoretical investigations (Slater and Villeneuve, 1992; Desruisseaux and Slater, 1994, 1996; Défontaines and Viovy, 1991, 1993, 1994; Slater et al., 1995) and a more recent experimental study (Desruisseaux et al., manuscript submitted for publication)

Received for publication 18 March 1998 and in final form 4 June 1998.

Address reprint requests to Dr. Gary W. Slater, Department of Physics, University of Ottawa, 150 Louis-Pasteur, Ottawa, Ontario, Canada K1N 6N5. Tel.: 613-562-5800, ext. 6775; Fax: 613-562-5190; E-mail: gary@physics.uottawa.ca.

© 1998 by the Biophysical Society

0006-3495/98/09/1228/09 $2.00

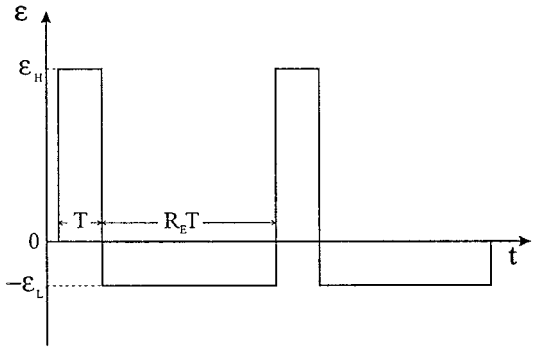

FIGURE 1 Time profile of the applied electric field for zero-integrated field electrophoresis (ZIFE). Here ϵ_H and ϵ_L denote the high and low field intensities, respectively, and the ratio R_E is given by $R_E = \epsilon_H/\epsilon_L$. The duration of one complete period is thus $(1 + R_E)T$, and the mean field is zero.

have demonstrated that TE suffers from an explosive increase of the diffusion coefficient. It is still unclear whether one can use pulsed fields (a reverse pulse is clearly an efficient way to detrap molecules) to improve the situation (Ulanovsky et al., 1990; Desruisseaux and Slater, 1996; Défontaines and Viovy, 1994).

Serwer's group studied various problems related to the gel electrophoretic migration of DNA molecules that carry a bulky object (Serwer et al., 1992; Serwer and Griess, 1993). In a recent abstract, Griess and Serwer (1998) presented a simple ratchet idea for the separation of a naked DNA from an identical DNA molecule that carries a bulky object (in the rest of this paper, this will be called an S-DNA complex, and the object will be called the label). These authors subjected a mixture of DNA and S-DNA to a ZIFE-like pulse sequence. They observed that the DNA was moving in the direction of the high field pulses, whereas the S-DNA was moving in the opposite direction. As mentioned above, these two effects are due qualitatively to nonlinearities and trapping, respectively.

In this article we present the first theoretical analysis of this original macromolecular separation technology for a case in which the label is attached at one end of the DNA (a similar theory can be derived for other cases). We first examine the general features (i.e., the possible operating regimes) of the process for zero-frequency and low-frequency pulses. This analysis is model-independent and uses only the well-known electrophoretic properties of DNA and the known TE results. We then use computer simulations to obtain quantitative results within the framework of the biased reptation model (BRM). Finally, we draw conclusions about the possible usefulness of this novel idea.

GENERAL THEORETICAL PRINCIPLES

Electrophoresis of a DNA molecule in a DC electric field

It is well known that when the electric field is low enough, long reptating DNA molecules retain their random walk conformations (see Fig. 2 *c*) during the electrophoretic migration. This is the linear regime characterized by a field-independent mobility μ. Heller et al. (1994), for example, have clearly established this behavior for double-stranded DNA electrophoresed in agarose gels. When the field ϵ exceeds a critical reptation value ϵ_R, however, the molecule becomes oriented in the field direction (Fig. 2 *a*) (Holzwarth et al., 1987). This orientation reduces the retarding effect of the gel. The mobility then becomes field-dependent ($\mu(\epsilon)$ is a monotonically increasing function of ϵ; see Fig. 3 *a*).

Electrophoresis of an S-DNA molecule in a DC electric field

If it were not for steric trapping, S-DNA complexes would have the same general electrophoretic properties as naked DNAs (except for an extra friction coefficient, which we will denote by α; in other words, the streptavidin has a friction coefficient equivalent to that of a DNA fragment containing α monomers). However, DNA reptation leads to situations such as the one shown in Fig. 2 *b*. In this case, the bulky object cannot follow the reptating molecule because the latter previously chose a tube section that was too narrow for the S-label. The oriented (Fig. 2 *b*) S-DNA molecule is thus trapped, because it is normally the charged DNA head that drives the migration. If the field is low enough, i.e., lower than a trapping critical value ϵ_T, trapping is of little importance because the Brownian forces dominate the electric forces and S-DNA molecules detrap very easily (Fig. 2 *d*). Because previous experimental investigations have demonstrated that $\epsilon_T < \epsilon_R$ in practice (Ulanovsky et al., 1990; Desruisseaux et al., manuscript submitted for publication), the mobility is field-independent in this

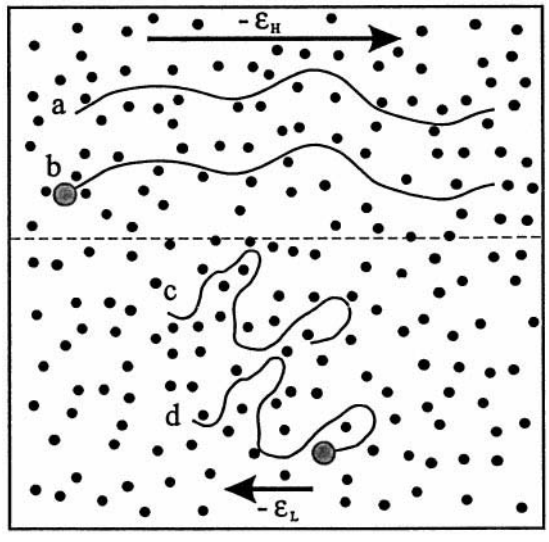

FIGURE 2 Schematic picture of the gel network (*black dots*); *b* and *d* show a protein-DNA complex (or S-DNA); *a* and *c* show a free DNA chain. In *c* and *d* the chains are in a low electric field, whereas the field is high for *a* and *b*. Note that the S-DNA molecule in *b* is trapped.

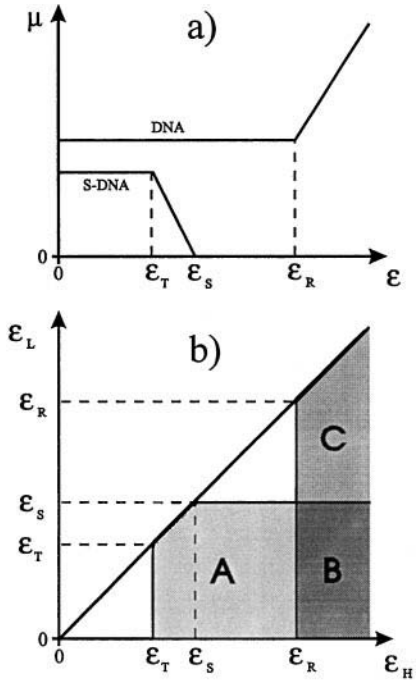

FIGURE 3 (*a*) A schematic drawing of the electrophoretic mobility μ for DNA and S-DNA molecules as a function of field strength ϵ. For DNA, the mobility is practically constant for $\epsilon < \epsilon_R$ and increases linearly with field beyond this value. For S-DNA, the mobility is constant up to $\epsilon = \epsilon_T$, then decreases quickly and becomes negligible for $\epsilon > \epsilon_S$. (*b*) Phase diagram for the zero-frequency ZIFE ratchet process. The net velocity of S-DNA is negative in regions A and B (and zero elsewhere), and the velocity of DNA is positive in regions B and C (and zero elsewhere).

weakly trapping regime (Fig. 3 *a*). When $\epsilon > \epsilon_T$, however, trapping becomes a serious problem, and the mobility quickly decreases with electric field because the electric forces actually hinder detrapping by Brownian motion. Finally, when the field exceeds the stopping critical value ϵ_S, the velocity is negligible, because the detrapping time is larger than the duration of the experiment (Fig. 3 *a*). In practice, we previously found that the critical fields ϵ_T and ϵ_S are very close (Desruisseaux et al., manuscript submitted for publication).

ZIFE-like pulses: the zero-frequency limit

Given the DC behavior of DNA and S-DNA described in Fig. 3 *a*, it is relatively easy to understand the dynamics of these molecules in the zero-frequency limit, because the transient behavior upon field reversal is then irrelevant. In other words, we can consider that the molecules instantaneously attain their steady-state mobility and diffusion coefficient after the field direction is changed.

Let us now discuss the effect of the type of pulsed field (called ZIFE) shown in Fig. 1. The high-field pulse of intensity ϵ_H is of duration T, and the reverse pulse of intensity $-\epsilon_L$ is of duration $R_E T$, where $R_E = \epsilon_H/\epsilon_L$ is the field ratio ($R_E > 1$). Note that this automatically implies that the mean field intensity $\langle E \rangle = 0$. The net velocity of a molecule (either DNA or S-DNA) is then given by

$$V = \frac{\epsilon_H \mu(\epsilon_H) - R_E \epsilon_L \mu(\epsilon_L)}{1 + R_E} = \frac{\epsilon_H}{1 + R_E} \times [\mu(\epsilon_H) - \mu(\epsilon_L)]. \quad (1)$$

The choice of the field intensities ϵ_H and ϵ_L is crucial for the two opposing ZIFE ratchets because of the presence of the differential mobility $\Delta\mu = \mu(\epsilon_H) - \mu(\epsilon_L)$ in Eq. 1.

It is clear that normal DNA will indeed have a net (positive) velocity unless both field intensities are lower than ϵ_R, in which case $\Delta\mu = 0$. Therefore, a sufficient condition for DNA to have a net velocity is $\epsilon_H > \epsilon_R$. This process was shown to be useful for the separation of chromosomal DNA (Turmel et al., 1990).

It is obvious that the net velocity of a S-DNA molecule will be zero if both fields are either lower than ϵ_T (in which case $\mu(\epsilon_H) = \mu(\epsilon_L)$) or higher than ϵ_S (mobility is zero in both directions). Otherwise, the net velocity will be negative because $\Delta\mu \leq 0$ in the presence of trapping. The most efficient situation is found when $\epsilon_H \gg \epsilon_S$ and $\epsilon_L \lesssim \epsilon_T$.

Fig. 3 *b* shows a "phase diagram" describing the net zero-frequency ZIFE velocities for DNA and S-DNA molecules with the same number of nucleotides. Both velocities are zero in the nonshaded areas (only the regions below the $\epsilon_H = \epsilon_L$ line are considered because $\epsilon_L \leq \epsilon_H$). In region A, the velocity of the S-DNA molecule is negative, whereas that of DNA is zero. In region B, the velocity of the S-DNA molecule is negative and the DNA velocity is positive. Finally, the velocity of the S-DNA molecule is zero and the DNA velocity is positive in region C. Obviously, one would have more regimes if the DNA critical field ϵ_R were smaller than ϵ_T (see Discussion), but it would still be easy to draw the corresponding phase diagram.

FINITE BUT LOW FREQUENCIES

Transients upon field reversal: DNA

We must first examine what happens to a DNA molecule immediately after the field direction (and intensity) changes. Immediately after the field is reversed from ϵ_H to $-\epsilon_L$, with $\epsilon_H > \epsilon_L$, the DNA molecule has an orientation corresponding to the field ϵ_H (Fig. 2 *a*), but must migrate in a field of intensity ϵ_L. Consequently, the molecule's velocity is higher at the beginning of the pulse ($V = -\mu(\epsilon_H)\epsilon_L$) and decreases as the molecule loses some of its orientation. Finally, the molecule reaches its steady-state velocity $V = -\mu(\epsilon_L)\epsilon_L$. Such field reversals are often characterized by velocity oscillations and overshoots (Sabanayagam and Holzwarth, 1996), but these effects can be neglected in our study, because we assume that the pulse duration is long compared to the time scales over which they appear.

If we now reverse the field back from $-\epsilon_L$ to $+\epsilon_H$, the molecule first has the (low) orientation corresponding to the field $-\epsilon_L$ (Fig. 2 *c*) and a velocity $V = +\mu(\epsilon_L)\epsilon_H$, but eventually orients in the (high) field direction and reaches

its steady-state velocity $V = +\mu(\epsilon_H)\epsilon_H$. Here again, we will neglect the velocity oscillations.

The dashed lines of Fig. 4 show a schematic plot of mean position $|\langle x\rangle|$ versus ϵt for a DNA molecule (note that because $\alpha = 0$ for naked DNA, the ordinate axis is simply $|\langle x\rangle|$). The time axis has been rescaled with the field intensity to directly compare the two parts of the ZIFE pulses (indeed, we note that we have $\epsilon t = \epsilon_H T$ at the end of the high-field pulse, whereas $\epsilon t = \epsilon_L R_E T = \epsilon_H T$ at the end of the low-field pulse). Moreover, the slopes give directly the mobilities on this type of diagram. In this case, we chose $\epsilon_H > \epsilon_R > \epsilon_L$. Curve a is for the high-field pulse, and curve c is for the low-field pulse. When the pulse duration $T < T^*$, the net velocity is predicted to be negative (i.e., in the direction of ϵ_L); this prediction has yet to be tested experimentally. In practice, however, times $T > T^*$ are more likely, and the net velocity of the DNA molecule will be positive (i.e., in the direction of the high-field pulses).

Transients upon field reversal: S-DNA

The behavior of the S-DNA molecule is expected to be similar to that of the DNA molecule for very short times (Fig. 4, *solid curves*). Here we have chosen $\epsilon_S > \epsilon_H > \epsilon_T > \epsilon_L$, so that the molecule is trapped only in the high field direction. Because the hydrodynamics friction coefficient of the uncharged label slows down the S-DNA molecule, we have rescaled the ordinate axis by the factor $(N + \alpha)/N$ to be able to superimpose the DNA and S-DNA curves. Note that if the molecules do not orient (low fields), there is no difference between DNA and S-DNA (besides the trivial rescaling of the position axis).

The dynamics of S-DNA in high fields $\epsilon_S > \epsilon_H > \epsilon_T$ is quite different, because trapping then dominates. Not long after it has reoriented in the high field direction, the S-DNA molecule becomes trapped and stops moving for a long (but finite) period of time. The most remarkable thing is that lines b (high field) and d (low field) cross twice: first for very short pulses (like naked DNA) because of the reorientation process described before for DNA, and then for much longer pulse durations $T = T^{**}$. Therefore, we predict that the net ZIFE velocity of the S-DNA molecules will change sign twice as the pulse duration is increased. The situation for $T \ll T^*$ (high-frequency pulses) will not be discussed, because it is both experimentally irrelevant and theoretically model-dependent.

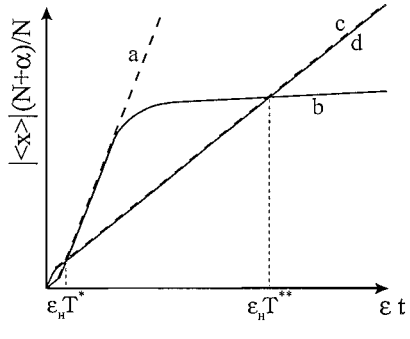

FIGURE 4 Schematic plot of the (modified) mean position $|\langle x\rangle|(N + \alpha)/N$ versus time ϵt for DNA (– – –) (note that $\alpha = 0$ in this case) and S-DNA (——), and for low (*c* and *d*) and high (*a* and *b*) field strengths.

SIMULATION RESULTS

The biased reptation model

Although the BRM's (Lumpkin et al., 1985; Slater and Noolandi, 1986; Slater, 1993) weaknesses have been well documented (Duke et al., 1994), this model still represents a useful tool for understanding the physics of gel electrophoresis processes, at least qualitatively. As we will see, the model-independent analysis presented in the previous sections agrees with the results of the BRM. We have thus used the simulation method developed previously by Slater and Villeneuve (1992) to study TE. Briefly, this modified BRM algorithm is as follows (see Slater, 1993, for more details).

The polyelectrolytes move by reptating between the gel obstacles. The electric forces bias both the motion inside the reptation tube as well as the mean orientation of the tube itself. Each curvilinear displacement of length $\pm a$ (a is the mean pore size) is of duration (Slater et al., 1987)

$$\tau(h_x) = \tau_B \times \frac{\tanh(\delta(h_x))}{\delta(h_x)}. \quad (2)$$

where h_x is the end-to-end distance of the DNA molecule in the field direction (x), $\tau_B = a^2/2D_c$ is the Brownian time for the unbiased (field $E = 0$) case, $D_c = k_B T/\xi(N + \alpha)$ is the curvilinear diffusion coefficient of the polymer in its reptation tube, $\delta = \epsilon\, h_x/a$ is the bias factor, $\epsilon = qEa/2k_BT$ is the scaled (dimensionless) electric field intensity, and q and ξ are, respectively, the charge and the friction coefficient of a primitive reptation segment of length a. These jumps occur with probabilities (Slater et al., 1987)

$$p_{\pm} = \frac{1}{1 + \exp[\mp 2\delta(h_x)]}, \quad (3)$$

where the $\pm$ refers to the (arbitrarily chosen) direction of the motion inside the tube. A new tube section of length a is created after each "jump" of duration τ. If a tube section is created by a charged end segment of the polymer chain, its orientation is biased by the field and follows a Boltzmann distribution function $\exp(-\epsilon \cos\theta)$, where θ is the angle between this new tube section and the field axis (Lumpkin et al., 1985; Slater and Noolandi, 1986). Tube sections created by the uncharged S end are randomly oriented.

The BRM has to be modified to take into account the S-DNA steric trapping that occurs when the label faces a small opening (Fig. 2). A fraction $f \ll 1$ of the pore-to-pore passages are thus marked "too narrow," and any move that tries to make the label move through such passages is rejected (however, the time τ is added to the current time).

Trapping occurs when the label is pinned by a narrow passage, and detrapping requires the molecule to move backward over a curvilinear distance $L = Na$ (the contour length of the reptation tube), where N is the number of reptation segments forming (or number of gel pores occupied by) the molecule. This detrapping process is the only one allowed by reptation (Desruisseaux and Slater, 1994, 1996; Slater and Villeneuve, 1992; Défontaines and Viovy, 1991, 1993, 1994; Slater et al., 1995). Because the bias factor $\delta = \epsilon h_x/a$ depends on both the field ϵ and the end-to-end distance h_x, detrapping is very unlikely for high field intensities and long, oriented molecules.

The simulations were carried out on Unix workstations using a Fortran code. The following conditions were used for the simulations: molecular size of the DNA molecules, $N = 20$; fraction of small pores, $f = 0.001$; high field intensity, $\epsilon_H = 1.0$; low field intensity, $\epsilon_L = 0.04$, so that $R_E = 25$. Note that for this molecule, $\epsilon_R \approx 0.84$ and $\epsilon_T \approx \epsilon_S \approx 0.05$ (Slater and Villeneuve, 1992). For simplicity, we chose $\alpha = 0$, so that it would easier to compare the results for DNA and S-DNA (for the streptavidin-DNA complex, α was found to be smaller than unity; Desruisseaux et al., manuscript submitted for publication). Therefore, the distances are measured in units of the mean pore size a, and the times are measured in units of τ_B. Note that $\tau_B \propto 1/D_c \propto N$ with these units. The high-field pulse ϵ_H defines the positive direction of migration.

The effect of frequency

Fig. 5 shows how the mean (steady-state) velocity of DNA (*squares*) and S-DNA (*circles*) varies as a function of the pulse duration T, and Fig. 6 shows a similar plot for the net diffusion coefficient. Remarkably, the S-DNA diffusion coefficient has a large maximum around $\log_{10} T \simeq 2.8$, but is actually lower than that of DNA for $\log_{10} T \lesssim 1$ and $\log_{10} T \gtrsim 4$.

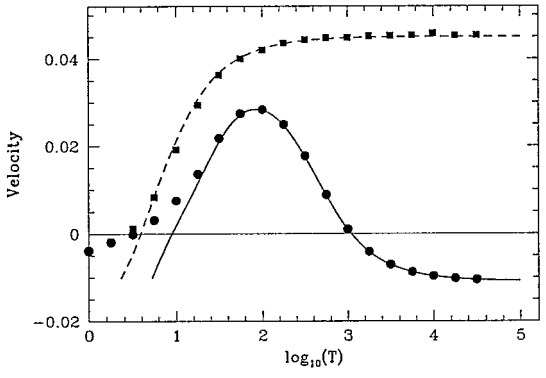

FIGURE 5 Mean electrophoretic velocity for DNA (■, – – –) and S-DNA (●, ——) as a function of pulse duration T. The simulation parameters used for Figs. 4–10 are described in the text. The data points come from the simulations, and the lines come from a simple theory that is also described in the text.

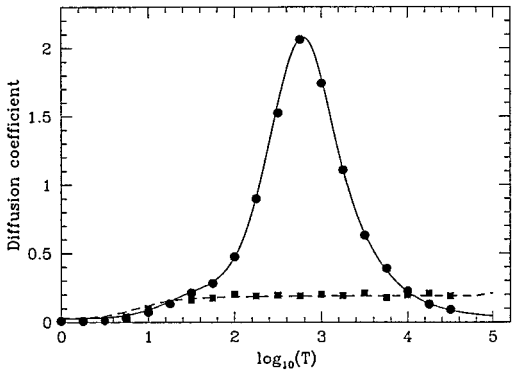

FIGURE 6 Diffusion coefficient for DNA (■, – – –) and S-DNA (●, ——) as a function of pulse duration T. The data points come from the simulations, and the lines come from a simple theory.

The dotted line in Fig. 5 represents the DNA velocity calculated using the constant field approximation and Fig. 4. To obtain this curve, two simulations in constant field were performed, one at $-\epsilon_L$ and one at ϵ_H. In both cases, we first oriented the molecules with respect to the other field to reproduce the conditions observed after a field reversal. The distance migrated during a high field pulse of duration T is $x_H(T) > 0$, and the distance migrated during the next low field pulse is $x_L(R_E T) < 0$. The total duration of a complete cycle is given by $(1 + R_E)T$. The steady-state velocity is thus given by

$$V_{ss}(T) = \frac{x_H(T) + x_L(R_E T)}{(1 + R_E)T}. \quad (4)$$

The solid line plotted on Fig. 5 represents the same calculation for S-DNA molecules. We note that the constant field approximation method is valid for $\log_{10} T > 1$ for DNA and for $\log_{10} T > 1.5$ for S-DNA. This simply reflects the fact that for pulses that are too short, the molecules do not have time to completely lose the orientation acquired during the previous pulse. Note that the label makes the S-DNA reorientation time longer, because this molecule must do a complete flip-flop after every field reversal, whereas a DNA molecule has perfect head/tail symmetry.

The dotted line in Fig. 6 represents the diffusion coefficient estimated by the same approach. The increase in the variance during the high field pulse is $\Delta x_H^2(T)$, whereas it is equal to $\Delta x_L^2(R_E T)$ during the low field pulse that follows. The resulting diffusion coefficient is then simply equal to

$$D_{ss}(T) = \frac{\Delta x_H^2(T) + \Delta x_L^2(R_E T)}{2(1 + R_E)T}. \quad (5)$$

The solid line represents the same calculation for S-DNA molecules. The two lines provide excellent approximations for $\log_{10} T > 1.5$. It should be mentioned that the constant field approximation can be used for any system in which it is possible to estimate the initial state (at the beginning of every pulse) of the system.

Fig. 7 shows a log-log plot of mean position $|\langle x\rangle|$ versus modified time ϵt during a high-field (*thick lines*) and low-field (*thin lines*) pulse for DNA (*dotted lines*) and S-DNA (*solid lines*). As discussed above, the net velocity of DNA and S-DNA is null when their two corresponding curves are crossing. Here we see that the curves for DNA are crossing once for $\log_{10} T \approx 0.6$, whereas the curves for S-DNA are crossing twice for $\log_{10} T \approx 1$ and $\log_{10} T \approx 3$. This is consistent with the schematic representation of Fig. 4 (which was not log-log).

Fig. 8 presents a log-log plot of the variance $|\Delta x^2|$ versus time ϵt during a high-field (*thick lines*) and low-field (*thin lines*) pulse for DNA (*dotted lines*) and S-DNA (*solid lines*). These curves are very useful for understanding the peak observed around $\log_{10} T = 2.8$ on Fig. 6. During a high-field pulse, the variance of the S-DNA band first increases very quickly for times $\log_{10} T < 2.8$, and plateaus for $\log_{10} T > 3$. The fact that the diffusion coefficient increases for $\log_{10} T < 2.8$ is due to the fact that $\Delta x^2 \propto t^\gamma$ with $\gamma > 1$, in this regime; see Desruisseaux and Slater (1994) for a study of the anomalous diffusion properties of S-DNA. The diffusion coefficient then decreases with T for $\log_{10} T > 3$, because $\Delta x^2 \propto t^0$ (no increase) when there is complete trapping. The DNA diffusion coefficient is constant for $\log_{10} T > 2$, because we then have $\Delta x^2 \propto t$ (normal diffusion) during both the high-field and low-field pulses.

Asymmetry of the DNA and S-DNA bands

The very peculiar asymmetrical dynamics of the S-DNA molecules in the system under investigation naturally leads to asymmetrical bands. The central-limit theorem, however, implies that the band shape should become Gaussian, and hence symmetrical, for long enough times. To investigate the band asymmetry and its temporal evolution, we also computed the band skew (Sk):

$$\mathrm{Sk} = \frac{\langle (x - \langle x\rangle)^3\rangle}{(\langle x^2\rangle - \langle x\rangle^2)^{3/2}}. \tag{6}$$

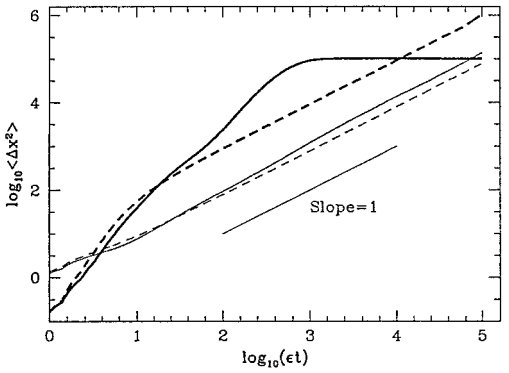

FIGURE 8 Log-log plot of band variance Δx^2 versus ϵt for DNA (*dashed lines*) and S-DNA (*solid lines*) during the high (ϵ_H; *thick lines*) and low (ϵ_L; *thin lines*) field pulses.

One thus has Sk = 0 for a symmetrical band, Sk < 0 for a band with a back tail, and Sk > 0 for one with a front tail. Fig. 9 shows Sk versus time for both DNA (*dashed lines*) and S-DNA (*solid lines*), and for pulse durations $\log_{10} T$ = 1, 2, 3, and 4. Note that the simulation conditions are identical to those used for Figs. 5 and 6, and that the initial band was a delta peak. The direction of the high field (ϵ_H) defines the positive ($+x$) direction of migration, and the pulse sequence starts with a high-field pulse.

The short time evolution of the S-DNA band skew is a function of the initial conditions (i.e., whether we start with a high-field or low-field pulse, and whether the molecules are initially relaxed or oriented). However, many characteristic results are independent of the initial conditions. For very long pulses (e.g., $\log_{10} T = 4$), the skew first goes up for $t < 3$ (a few molecules start moving), then down (the rest of the molecules complete their very first move; note that the skew is then negative!), and then up again (some molecules are left behind in very deep traps), before it saturates (all molecules have fallen into deep traps). The field reversal at $\log_{10} t = 4$ frees the molecules, and the skew slowly decreases as $t^{-1/2}$ for very long times (more than 100 pulses), as expected for a simple directed walk

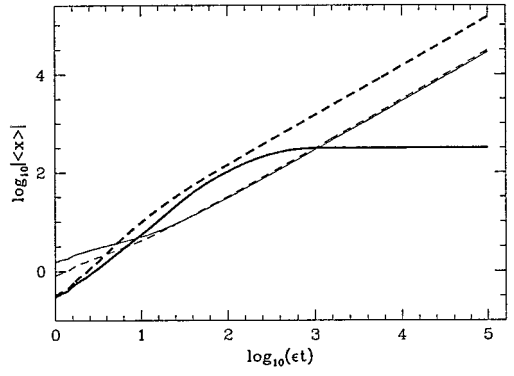

FIGURE 7 Log-log plot of the mean position $|\langle x\rangle|$ versus ϵt for DNA (*dashed lines*) and S-DNA (*solid lines*) during the high (ϵ_H; *thick lines*) and low (ϵ_L; *thin lines*) field pulses.

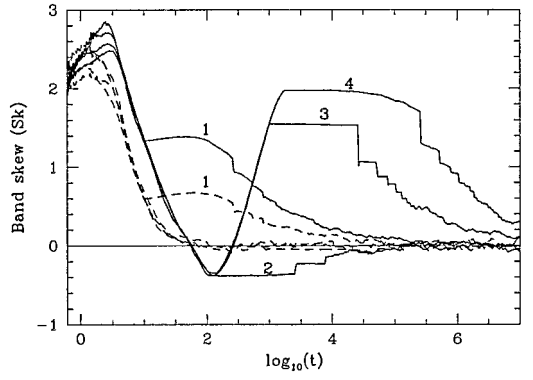

FIGURE 9 Band skew (Sk) for DNA (– – –) and S-DNA (——) as a function of time t for pulse durations $\log_{10} T$ = 1, 2, 3, and 4, as indicated. The dashed curves (DNA) are almost identical for $\log_{10} T$ = 2, 3, and 4.

problem (see Appendix A). The situation is quite similar for $\log_{10} T = 3$. In comparison, the skew goes down to zero very quickly for DNA (the initial peak is due to the fact that we have a wide distribution of tube renewal times in the presence of a field, a distribution that is related to the distribution of end-to-end distance h_x). For $\log_{10} T = 1$, on the other hand, the evolution of the skew is almost identical for S-DNA and DNA, because the pulse duration is shorter than both the mean time between traps and the mean tube renewal time.

The situation for $\log_{10} T = 2$ is qualitatively different. Because the pulse duration T is now comparable to the mean time between traps, the skew remains negative (but small) after the initial decay. This is an interesting phenomenon, and it provides a simple experimental method for estimating the mean trapping time.

The resolution between DNA and S-DNA

There are many ways to mathematically express the resolution between two bands. One popular definition of resolution (R) is given by (Giddings, 1991)

$$R = \frac{|\langle x_1 \rangle - \langle x_2 \rangle|}{2(\sigma_1 + \sigma_2)}, \tag{7}$$

where $\langle x_1 \rangle$ and $\langle x_2 \rangle$ are the center of mass positions of bands 1 and 2, respectively, and σ_1 and σ_2 are the standard deviations of these bands. The resolution between two bands normally grows like $R \propto t^{1/2}$. In such cases, $R/t^{1/2}$ is a fundamental parameter that tells us how fast two bands are being resolved from each other (large values of $R/t^{1/2}$ means that less time will be required to resolve the bands). Fig. 10 shows the resolution ratio $R/t^{1/2}$ between a naked DNA molecule and the corresponding S-DNA molecule versus pulse duration T. The data points come from our Monte Carlo simulations, whereas the solid line was obtained using the constant field approximation discussed previously.

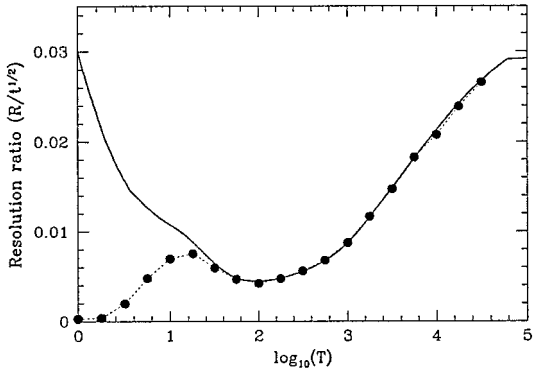

FIGURE 10 Resolution ratio $R/t^{1/2}$ versus pulse duration T for the ratchet separation between a DNA band and the corresponding S-DNA band. The solid line comes from the simple theory described in the text. The dotted line connects the data points obtained from the pulsed-field simulations.

Clearly, long pulse durations are preferable. Again, the critical value $\log_{10} T \simeq 2$ shows up as a minimum.

DISCUSSION

This article establishes the general theoretical framework that is necessary to understand and explain the results of the Griess and Serwer ratchet electrophoretic separation process for S-DNA and DNA molecules. For the sake of simplicity, we have focused our study on the following conditions: 1) the label (S) is attached at the end of the DNA molecule; 2) the reptation orientation field ϵ_R is higher than the trapping field ϵ_T ($\approx \epsilon_S$); 3) the pulse frequency is small compared to the frequency of the intramolecular DNA stretching and relaxation modes. Clearly, a model that would cover all possible cases would lead to an essentially infinite number of separation regimes, and hence would be useless at this stage. The theoretical approach described in this article will easily be adapted to other situations once more detailed experimental data become available.

We have shown that such ratchets should be using very low frequencies to optimize resolution. However, the pulse duration can also be used as a spectroscopic tool to estimate the microscopic times, such as the mean trapping and detrapping times. For instance, the mean S-DNA velocity is predicted to change sign (and its diffusion coefficient to reach a maximum value) for intermediate pulse durations that correspond closely to these characteristic times. We have also demonstrated that this trapping mechanism should lead to asymmetrical bands, and that the latter should slowly become symmetrical over hundreds of pulses.

The field dependence of the gel electrophoretic mobility of charged spherical particles is qualitatively different from that of DNA because particles do not "orient" in the field (i.e., their mobility is essentially constant in the absence of trapping). In the presence of trapping, however, their behavior is somewhat similar to that of S-DNA, i.e., their mobility vanishes beyond a certain critical field intensity (Griess and Serwer, 1990; Serwer, 1993; To and Boyde, 1993). With zero-frequency ZIFE-type pulses, particles can have either a zero net velocity (if they are not trapped in either direction), or a net negative velocity (if they are trapped in the positive—high field—direction). At high frequency, the net velocity of trapped particles should actually be zero when the pulse duration T becomes smaller than the time it takes to fall into a dead end (trap). The only way to make particles move in opposite directions would thus be to slightly bias the pulsed field, as described previously for a different system (Slater et al., 1997).

The first part of the paper described general model-independent principles that apply to S-DNA ratchets. The second part used a specific electrophoresis model (the BRM) for computer simulation purposes. The BRM has largely been replaced by the BRF (biased reptation model with fluctuations) over the last few years. The main difference between the two is that the latter correctly predicts that

the mobility of DNA should increase linearly with field intensity when $\epsilon > \epsilon_R$ in most experimental situations, whereas the first predicted a quadratic increase (Duke et al., 1994; Semenov et al., 1995). Thus the qualitative predictions of the simulation results are not affected by this difference. Neither model would correctly describe the dynamics at very high frequencies.

Perhaps the most important problem not treated in our study is that of DNA/S-DNA mixtures. For example, can this ratchet process separate many DNA and S-DNA molecules of different lengths simultaneously? Can this ratchet separate S-DNA molecules of identical lengths but different anchoring points for the bulky S-label? Can it separate S-DNA molecules with more than one label?

The Griess and Serwer ratchet process is very flexible and can be modified in many ways. For example, the pulse shape (which does not have to be square), frequency, and amplitude (both of which can be changed during the separation) offer tunable parameters. Moreover, one can add a small DC component to the ZIFE pulses to bias the separation process toward a given direction (this can easily increase the efficiency). More interesting, however, would be two-dimensional schemes in which different separation conditions are used in two orthogonal directions. We are currently looking at how one could potentially use these "experimental degrees of freedom" to achieve the goals described in the previous paragraph.

APPENDIX A: THE DIRECTED WALK PROBLEM

The motion of our polylectrolytes during one complete pulse cycle is similar to that of a particle that makes a jump over a distance $x \geq 0$ (the displacement during the cycle) every time unit (the cycle duration). Let $P(x)\mathrm{d}x$ be the probability distribution function for these jumps. The mean velocity of the particle is then simply given by $V = \langle x \rangle$. It is easier to calculate the moments of the distribution of particles after t jumps if we use the relative position $s = x - \langle x \rangle$, such that the mean position of the particles is always $s = 0$. The problem is then reduced to evaluating the variance $\langle (x - \langle x \rangle)^2 \rangle = \langle s^2 \rangle$ and third moment $\langle (x - \langle x \rangle)^3 \rangle = \langle s^3 \rangle$. Indeed, after t independent (i.e., uncorrelated) jumps, the mean position is given by

$$\langle S(t) \rangle = \left\langle \sum_{i=1}^{t} s_i \right\rangle = t\langle s \rangle = 0, \tag{A1}$$

where the moments of s are defined by

$$\langle s^j \rangle = \int_{-\langle x \rangle}^{\infty} P(s) s^j \, \mathrm{d}s. \tag{A2}$$

The second moment of the distribution of final positions $S(t)$ is

$$\langle S^2(t) \rangle = \left\langle \left(\sum_{i=1}^{t} s_i \right)^2 \right\rangle = \left\langle \sum_{i=1}^{t} s_i^2 + \sum_{i}^{t} \sum_{j \neq i}^{t} s_i s_j \right\rangle. \tag{A3}$$

Because the jumps are uncorrelated, the last term is zero and we obtain

$$\langle S^2(t) \rangle = t\langle s^2 \rangle \propto t. \tag{A4}$$

Similarly,

$$\langle S^3(t) \rangle = \left\langle \left(\sum_{i=1}^{t} s_i \right)^3 \right\rangle = \left\langle \sum_{i=1}^{t} s_i^3 + 3 \sum_{i \neq j} s_i^2 s_j + \sum_{i \neq j \neq k} s_i s_j s_k \right\rangle = t\langle s^3 \rangle \propto t. \tag{A5}$$

Therefore, the skew $\langle (x - \langle x \rangle)^3 \rangle / \langle (x - \langle x \rangle)^2 \rangle^{3/2} = \langle S^3 \rangle / \langle S^2 \rangle^{3/2} = \Gamma / t^{1/2}$, where $\Gamma = \langle s^3 \rangle / \langle s^2 \rangle^{3/2}$ is a time-independent property of the probability distribution function $P(x)dx$. Note that the skew is zero for a symmetrical distribution function, as it should be. For an asymmetrical distribution function, the skew will thus decrease as $1/t^{1/2}$, and the band will become symmetrical for long enough times.

The authors thank Dr. P. Serwer for sending us preprints before publication.

This work was supported by a research grant of the National Science and Engineering Research Council of Canada to GWS. One of the authors (TBLK) acknowledges the fellowship from CNPq-Brazil, as well as the stimulating and profitable work environment in the Departments of Physics and Biology of the University of Ottawa.

REFERENCES

Andrews, A. T. 1986. Electrophoresis: Theory, Techniques and Biochemical and Clinical Applications. Clarendon, Oxford.

Astumian, R. D. 1997. Thermodynamics and kinetics of a Brownian motor. *Science.* 276:917–922.

Chacron, M. J., and G. W. Slater. 1997. Particle trapping and self-focusing in temporally asymmetric ratchets with strong field gradients. *Phys. Rev. E.* 56:3446–3450.

Chialvo, D. R., and M. M. Millonas. 1995. Asymmetric unbiased fluctuations are sufficient for the operation of a correlation ratchet. *Phys. Lett. A.* 209:26–30.

Défontaines, A. D., and J. L. Viovy. 1991. Theoretical model of trapping electrophoresis. *In* Proceedings of the First International Conference on Electrophoresis, Supercomputing and the Human Genome. World Scientific, Singapore. 286–313.

Défontaines, A. D., and J. L. Viovy. 1993. Gel electrophoresis of an end-labeled DNA. I. Dynamics and trapping in constant fields. *Electrophoresis.* 14:8–17.

Défontaines, A. D., and J. L. Viovy. 1994. Gel electrophoresis of end-labeled DNA. II. Dynamics and detrapping in pulsed fields. *Electrophoresis.* 15:111–119.

Desruisseaux, C., and G. W. Slater. 1994. Simple model of trapping electrophoresis with complicated transient dynamics. *Phys. Rev. E.* 49:5885–5888.

Desruisseaux, C., and G. W. Slater. 1996. Pulsed-field trapping electrophoresis: a computer simulation study. *Electrophoresis.* 17: 623–632.

Duke, T. A. J., T. E. Holy, and S. Leibler. 1995. "Gliding assays" for motor proteins: a theoretical analysis. *Phys. Rev. Lett.* 74:330–333.

Duke, T. A. J., J. L. Viovy, and A. N. Semenov. 1994. Electrophoretic mobility of DNA in gels. I. New biased reptation theory including fluctuations. *Biopolymers.* 34:239–247.

Dunn, M. J., and J. M. Corbett. 1996. Two-dimensional polyacrylamide gel electrophoresis. *Methods Enzymol.* 271:177–203.

Giddings, J. C. 1991. Unified Separation Science. John Wiley & Sons, New York. 90, 102.

Griess, A. G., and P. Serwer. 1990. Gel electrophoresis of micron-sized particles: a problem and a solution. *Biopolymers.* 29:1863–1866.

Griess, G. A., and P. Serwer. 1998. Gel electrophoretic ratcheting for the fractionation of DNA-protein complexes. *Biophys. J.* 74:A71.

Guttman, A. 1996. Capillary sodium dodecyl sulfate-gel electrophoresis of proteins. *Electrophoresis.* 17:1333–1341.

Heller, C., T. A. J. Duke, and J. L. Viovy. 1994. Electrophoretic mobility of DNA in gels. II. Systematic experimental study in agarose. *Biopolymers.* 34:249–254.

Holzwarth, G., C. B. Mckee, S. Steiger, and G. Crater. 1987. Transient orientation of linear DNA molecules during pulsed-field electrophoresis. *Nucleic Acids Res.* 15:10031–10044.

Jülicher, F., A. Ajdari, and J. Prost. 1997. Modelling molecular motors. *Rev. Mod. Phys.* 69:1269–1281.

Lumpkin, O. J., P. Déjardin, and B. H. Zimm. 1985. Theory of gel electrophoresis. *Biopolymers.* 24:1573–1593.

Magnasco, M. O. 1993. Forced thermal ratchets. *Phys. Rev. Lett.* 71: 1477–1481.

Rousselet, J., L. Salomé, A. Ajdari, and J. Prost. 1994. Directional motion of Brownian particles induced by a periodic asymmetric potential. *Nature.* 370:446–448.

Sabanayagam, C. R., and G. Holzwarth. 1996. Real-time velocity of DNA bands during field-inversion gel electrophoresis. *Electrophoresis.* 17: 1052–1059.

Semenov, A. N., T. A. J. Duke, and J. L. Viovy. 1995. Gel electrophoresis of DNA in moderate fields: the effect of fluctuations. *Phys. Rev. E.* 51:1520–1537.

Serwer, P., and G. A. Griess. 1993. Large particle gel electrophoresis. *Anal. Magazine.* 21:M16–M20.

Serwer, P., S. J. Hayes, E. T. Moreno, and C. Y. Park. 1992. A small (58-nm) attached sphere perturbs the sieving of 40–80-kilobase DNA in 0.2–2.5% agarose gels: analysis of bacteriophage T7 capsid-DNA complexes by use of pulsed field electrophoresis. *Biochemistry.* 31: 8397–8405.

Slater, G. W. 1993. Theory of band broadening for DNA gel electrophoresis and sequencing. *Electrophoresis.* 14:1–7.

Slater, G. W., C. Desruisseaux, C. Villeneuve, H. L. Guo, and G. Drouin. 1995. Trapping gel electrophoresis of end-labeled DNA: an analytical model for mobility and diffusion. *Electrophoresis.* 16:704–712.

Slater, G. W., H. L. Guo, and G. I. Nixon. 1997. Bidirectional transport of polyelectrolytes using self-modulating entropic ratchets. *Phys. Rev. Lett.* 78:1170–1173.

Slater, G. W., and J. Noolandi. 1986. On the reptation theory of gel electrophoresis. *Biopolymers.* 25:431–454.

Slater, G. W., J. Rousseau, and J. Noolandi. 1987. On the stretching of DNA in the reptation theories of gel electrophoresis. *Biopolymers.* 26:863–872.

Slater, G. W., and C. Villeneuve. 1992. A computer simulation of trapping electrophoresis. *J. Polym. Sci. B.* 30:1451–1457.

To, K.-Y., and T. R. C. Boyde. 1993. Pulsed-field acceleration: the electrophoretic behavior of large spherical particles in agarose gels. *Electrophoresis.* 14:597–600.

Turmel, C., E. Brassard, R. Forsyth, K. Hood, G. W. Slater, and J. Noolandi. 1990. High resolution zero integrated field electrophoresis of DNA. *In* Electrophoresis of Large DNA Molecules: Theory and Applications. E. Lai and B. W. Birren, editors. Cold Spring Harbor Laboratory, Cold Spring Harbor, New York. 101–131.

Ulanovsky, L., G. Drouin, and W. Gilbert. 1990. DNA trapping electrophoresis. *Nature.* 343:190–192.